Influence of titanium carbide on the interlaminar shear strength of carbon fibre laminate composites

A. Centeno[1], J.A.Viña[2], C. Blanco[1*], R. Santamaría[1], M. Granda[1], R. Menéndez[1]

[1]Instituto Nacional del Carbón (INCAR-CSIC), Apdo. 73, 33080-Oviedo, Spain

[2]Higher Technical School of Industrial Engineering of Gijón, University of Oviedo, 33204-Gijón, Spain

Abstract.-

The potential use of carbon fibre laminate composites is limited by the weak out-of-plane properties, especially delamination resistance. The effect of incorporating titanium carbide to the mesophase pitch matrix precursor of carbon fibre laminate composites on interlaminar shear strength is studied both on carbonised and graphitised composites. The presence of titanium carbide modifies the optical texture of the matrix from domains to mosaics in those parts with higher concentrations and it contributes to an increase of fibre/matrix bonding. This fact produces an increase of the interlaminar shear strength of the material and changes the fracture mode.

Keywords : A. Carbon fibres; A. Laminate ; B. Fracture ; B. Fibre/matrix bond ; B. Mechanical properties

1. INTRODUCTION

Corresponding author: Clara Blanco, e-mail: clara@incar.csic.es; Francisco Pintado Fe, 26 Apdo.73, 33080-Oviedo (Spain) Tel.: + 34 985 11 89 94; Fax.: +34 985 29 76 62

Different applications have been identified for carbon-based materials in fusion devices, aircraft braking systems, high temperature lubricants or air breathing propulsion systems. A common aspect in the material specifications for these applications is the need for very high thermal conductivity, thermal shock resistance and high excellent mechanical properties [1]. Carbon fibre reinforced composites (CC) achieve these requirements. However, the interlaminar shear strength (ILSS) is usually a limiting design characteristic of laminate composites. The fabrication process usually involves densification, carbonisation and high thermal treatment (graphitisation) [1]. During the processing, interlaminar cracks are formed mainly caused by the pressure of volatiles release during carbonisation and thermal stresses [1]. The failure between the different planes of the reinforcement layers (delamination) is the most critical failure mechanism of laminates. Therefore, the improvement of this property has been a relevant objective in this field of materials science. Some proposed alternatives are weaving fibres in the thickness direction (3D textiles) [2-4] and, more recently, the incorporation of carbon nanotubes in the woven [5-8]. Since the behaviour of the composites strongly depends on the fibre/matrix interfacial properties, several methods have been investigated in order to improve the degree of adhesion between them. Concerning fibres, a wide variety of surface modification [9,10] and coating methods [11] are often applied. Studies related to the modification of carbon matrix mainly focus on the combination of different types of matrix and microstructures [12,13] and only a few of them study the incorporation of fillers such as carbon black [14]. Meanwhile, there are many studies of methods to modify polymeric matrix composites, such as the incorporation of carbon

nanotubes [5,15] or the addition of nanoparticles to the matrix [16,17]. These methods, in principle, could also be valid for CC composites.

The measurement of the ILSS of a material requires a pattern of pure shear stress to be generated between laminates to induce an interlaminar shear failure. Some of the most common tests used for this propose are the Compression Shear Test (CST) [18], the Iosipescu test [19], the double-notch shear test (compression) [20], the four point flexural test [21] and the short beam shear test (SBS) [22,23]. SBS test is based on a transverse shear failure through three-point bending and is used as standard method for determining the interlaminar shear strength of fibre reinforced composites because of its simplicity [24,25]. The main drawback is that not all specimens fail in transverse shear and different failure modes can take place during fracture [22]. In spite of that, SBS is a good method for determining the apparent interlaminar shear strength and to compare the behaviour between materials with the same nature [24].

In a previous paper [26], the authors studied the influence of the addition of TiC nanoparticles on the thermal conductivity of CC laminates. The results obtained showed that the addition of a small proportion of these particles to the matrix precursor resulted in a significant increase of the thermal conductivity of the graphitised material. During graphitization mesophase-based carbon matrix achieves a high degree of order. This order is further developed with the addition of TiC due to its catalytic effect on carbon graphitization [27] and is responsible for the increae in the thermal conductivity observed. However there are no studies up to date regarding the influence of these nanoparticles on the mechanical properties on CC composites. Therefore, the aim of the present study is to evaluate the influence of TiC on the interlaminar shear strength of

these materials. The fracture behavior was evaluated on carbonized and graphitized composites attending to the number of densification cycles applied.

2. EXPERIMENTAL

Undoped and Ti-doped CC composites were prepared by liquid impregnation of 2D twill weave PAN-based carbon fibre preforms (60 % vol. fibres) using a commercial naphthalene derived mesophase pitch (AR) as matrix precursor. The Ti-doped matrix precursor was obtained by mixing 10 wt. % TiC nanoparticles (130 nm) with AR [28]. The experimental details used in the densification process have been previously described [29]. The composites were carbonised at 1000°C and the resultant materials were labeled as CCAR-C and CCTi-C, respectively for the undoped and titanium doped composites. Up to three densification-carbonisation cycles were applied in order to reduce the porosity. Finally, the materials were graphitised at 2700°C and correspondingly labeled as CCAR-G and CCTi-G. Characterization was performed both for the undoped and Ti-doped materials, for each densification cycle.

2.1 Characterization of CC composites

The open and close porosity of the materials were measured by Archimedes principle and helium pycnometry, respectively. The microstructure of the material and dopant distribution was studied by optical microscopy and scanning electron microscopy (SEM). The analysis of the chemical composition on specific areas of the Ti-doped materials was performed using an X-ray energy dispersive analyser (EDX). The interlaminar shear strength of the materials was determined using the short beam shear test method (SBS) following the ASTM standard D2344-00. The load was applied

perpendicular to the plane of the laminates on specimens with 30 mm length and 5 mm thickness. A loading roller of 7 mm and supporting roller of 4 mm were used. The machine cross-head speed was 1.3 mm min^{-1}. SEM analysis was used to study the fracture surfaces.

3. RESULTS AND DISCUSSION

The open porosity decreased after three densification cycles from 40 vol. %, which corresponds to the initial preform, to ~9 vol. % in carbonised materials (Table 1). Meanwhile, the close porosity increases with the densification cycles. This increase is attributed to volatiles released from the matrix during carbonisation and also to the difficultness for their release depending on the type of weaving, as pointed out by Manocha et al. [30]. Graphitised materials showed a slightly increase in their porosity (Table 1) as a result of the aperture of close porosity, related to the contractions that take place during graphitisation.

Ti content in CCTi-G with 3 densification cycles is 2.3 wt % with respect to the whole material, which is around 13 wt. % with respect to the matrix. The optical texture of the undoped matrix shows flow domains (Figure 1a), while that corresponding to the doped material is also composed by domains, where TiC is well distributed (position A in Figure 1b and Figure 1c) and by mosaics, features of smaller size, in those areas with higher amount of dopant, specially close to the intersections between bundles of fibres (position B in Figure 1b and Figure 1c). The microstructure of the materials and the dopant distribution was studied by SEM. The analysis showed a good dispersion of the dopant throughout the material (Figure 2a). The good bonding between matrix and fibres, both for the undoped and the Ti-doped carbonised materials, was maintained

after graphitization (Figure 2b). In Ti-doped carbonised materials, the carbide is fairly well distributed in the matrix with sub-micrometric size particles although occasionally also some larger agglomerates (~2μm) are observed (Figure 2c). After graphitisation, agglomerates of larger size (~5μm) were formed (Figure 2d) due to the movement of TiC in the carbonaceous matrix [27].

As could be expected, the interlaminar shear strength increases, both in the carbonized and graphitized materials, with the number of densification cycles applied due to the reduction of porosity and the presence of higher amount of matrix in the material (Table 1). The interlaminar shear strength of CCTi-C is ~20 % higher than that of the corresponding to undoped material (Table 1). The smaller microstructures developed in the doped matrix can play an important role in the improvement of the mechanical properties [31]. The fracture behaviour was also different due to the presence of the dopant. While a clear failure by delamination occurs for undoped materials with 2 densification cycles, a mixed mechanism flexure/shear takes place in the fracture of the doped materials. In doped materials, the permanent retention of the deformation leads to the onset of compression [24] and causes the contribution of flexure in the failure of the specimen, showing their higher interlaminar shear strength. SEM analysis of fracture surfaces also showed significant differences between both carbonized materials (Figure 3). In the undoped materials, the fracture surface of the laminate, where the failure occurred by shear (XY plane), showed a higher amount of fibres and matrix released from the surface (Figure 3a). Meanwhile, the doped materials showed less detachment of fibre from matrix (Figure 3b), demonstrating the better adherence between fibre and matrix due to the presence of the carbide.

In general, after graphitisation the strength values decreased with regard those obtained in carbonized materials (Table 1). This decrease is related to the increase of porosity and, therefore, to the presence of lower amount of matrix in the material that can not distribute so efficiently the load to the fibres. The presence of the dopant showed an improvement in the strength resistance. CCTi-G with 2 cycles showed an apparent interlaminar shear strength of 18 MPa, significantly higher than that obtained in CCAR-G (8 MPa). However, there was no clear effect of the dopant for those values obtained for the materials with 3 densification cycles. This is explained when the fracture behaviour of these materials is studied in detail. The trend of the load/displacement curves showed a radical change due to the presence of the dopant (Figure 4). While a gradual loss of the load after the maximum value is obtained for CCAR-G, typical of a pseudo-plastic behaviour as it was observed in all carbonised materials, a sudden drop of the load occurs in CCTi-G, exhibiting a brittle fracture. This behaviour seems to be related to the stronger bonding between fibre and matrix of the doped materials. The fracture behaviour of the specimens changed also rather significantly. The failure of CCTi-G with 3 densification cycles showed a flexure fracture, as can be observed in the specimen shown in Figure 4. In these materials the resistance between layers is so high that prevents the rupture by shear. Therefore, the value obtained for CCTi-G with 3 densification cycles (28 MPa) corresponds to the shear resistance of the entire laminate, while the value of interlaminar shear strength might be higher. This fact justifies that the values obtained for CCTi-G and CCAR-G with 3 cycles are not directly comparable, as the fracture mode is different. Meanwhile, in the undoped materials two phenomena occur. The first one is the separation between layers, which implies a failure by interlaminar shear (mode II) and, afterwards, the

layers fail independently (see specimen in Figure 4). SEM images of the surfaces fractured by shear (YZ plane) are shown in Figures 5a and b, corresponding to undoped and Ti-doped composites respectively. Remarkable differences between both materials can be observed. While in the undoped materials an easy debonding between matrix and fibre occurs (Figure 5a), this debonding is not observed in the doped materials as result of the stronger bonding between fibre and matrix (Figure 5b). The same trend was observed for the surface provoked by flexure (XZ plane) (Figure 6). The undoped materials showed a strong pull-out on the fracture surface (Figure 6a), indicating a weak bonding between fibre and matrix. Figure 6c shows a detail of the holes formed by matrix due to the pull-out of fibres. Meanwhile, the fracture surface of the doped materials showed a joint failure of fibre and matrix (Figure 6b), demonstrating the strong bonding between them. Figure 6d shows a greater detail of the joint failure fibre/matrix evidencing the strong bonding in Ti-doped materials.

4.- CONCLUSIONS

The presence of titanium carbide modifies the optical texture of the matrix from domains to mosaic in those areas with higher concentration and causes the improvement of the interlaminar shear strength of both the carbonised and graphitised materials. Interlaminar delamination was usually the dominant failure in the undoped materials. Meanwhile, Ti-doped materials showed a combination of flexure/shear in the failure mechanism due to their higher shear resistance. As result, the value obtained for CCTi-G with 3 densification cycles corresponds to the shear resistance of the entire laminate, while the value of interlaminar shear strength would be higher. As observed in the load-displacement curves corresponding to the graphitised materials, the Ti-doped material

failed catastrophically as a result of the stronger fibre/matrix bonding, clearly observed by SEM images of fracture surfaces, where doped materials showed a joint failure fibre/matrix unlike undoped materials which showed a strong pull-out.

Acknowledgements

This work has been performed within the framework of the Integrated European Project "ExtreMat" (contract NMP-CT-2004-500253) with financial support by the European Community and the Spanish Education Ministry (Programa Nacional de Cooperación Internacional de Ciencia y Tecnología, Acciones Complementarias, MAT2004-22787-E).

References

[1] E.Fitzer, L.M. Manocha. Carbon reinforcements and carbon/carbon composites. Berlin:Springer.(1998).

[2] S.K. Sharma, B.V. Sankar. Effect of stitching on impact and interlaminar properties of graphite/epoxi laminates. Journal Thermoplastic Composites Materials 10:241-253 (1997).

[3] J. Brandt, K. Drechsler and F. J. Arendts Mechanical performance of composites based on various three-dimensional woven-fibre preforms. Composites Science and Technology 56(3): 381-386. (1996).

[4] F. Stig and S. Hallström. Assessment of the mechanical properties of a new 3D woven fibre composite material. Composites Science and Technology 69(11-12): 1686-1692. (2009).

[5] A. Warrier, A. Godara, O. Rochez, L. Mezzo, F. Luizi, L. Gorbatikh, S. V. Lomov,

A. W. VanVuure and I. Verpoest. The effect of adding carbon nanotubes to glass/epoxy composites in the fibre sizing and/or the matrix. Composites Part A: Applied Science and Manufacturing 41(4): 532-538. (2010).

[6] Tsu-Wei Chou, Limin Gao, Erik T. Thostenson, Zuoguang Zhang, Joon-Hyung Byun. An assessment of the science and technology of carbon nanotube-based fibers and

Composites. Composites Science and Technology 70: 1-19. (2010).

[7] J. Zhu, A. Imam, R. Crane, K. Lozano, V. N. Khabashesku and E. V. Barrera Processing a glass fiber reinforced vinyl ester composite with nanotube enhancement of interlaminar shear strength. Composites Science and Technology 67(7-8): 1509-1517. (2007).

[8] S. S. Wicks, R. G. de Villoria and B. L. Wardle. Interlaminar and intralaminar reinforcement of composite laminates with aligned carbon nanotubes. Composites Science and Technology 70(1): 20-28. (2010).

[9] S. Marinkovic, S. Dimitruevic Carbon/carbon composites prepared by chemical vapour deposition. Carbon 23:691–699. (1985).

[10] K. Christ, K.J. Hüttinger. Carbon-fiber-reinforced carbon composites fabricated with mesophase pitch. Carbon: 31 (5): 731-750. (1993).

[11] Hariom Dwivedi, Rakesh B. Mathur,Tersem L. Dhami , Om P. Bahl, Marc Monthioux, Sahendra P. Sharma. Evidence for the benefit of adding a carbon interphase in an all-carbon composite. Carbon 44: 699-709. (2006).

[12] F. Dillon, K. M. Thomas, H. Marsh. The influence of the matrix microstructure on the mechanical properties of CFRC composites. Carbon 31:1337-1348 (1993).

[13] B. Reznik, M. Guellali, D. Gerthsen, R. Oberacker, M.J.Hoffmann Microstructure and mechanical properties of carbon–carbon composites with multilayered pyrocarbon matrix. Materials Letter 52: 14–19 (2002).

[14] G. Chollona, O. Sirona, J. Takahashia, H. Yamauchib, K. Maedab, K. Kosakab. Microstructure and mechanical properties of coal tar pitch-based 2D-C/C composites with a filler addition. Carbon 39:2065-2075 (2001).

[15] Z. Fan, M. H. Santare, S. G. Advani "Interlaminar shear strength of glass fiber reinforced epoxy composites enhanced with multi-walled carbon nanotubes.

Composites

Part A: Applied Science and Manufacturing 39(3): 540-554. (2008).

[16] N. Shahid, R. G. Villate and A. R. Barron. Chemically functionalized alumina nanoparticle effect on carbon fiber/epoxy composites. Composites Science and Technology 65(14): 2250-2258. (2005).

[17] N.A. Siddiqui, RCS Woo, J.K. Kim, CCK Leung, A. Munir. Mode interlaminar fracture behavior and mechanical properties of CFRPs with nanoclay-filled epoxi matrix, Composites part A: Applied science and manufacture 38 449-460 (2006).

[18] K. Schneider, B.Lauke, W.Beckert. Compression Shear Test (CST)- A Convenient Apparatus for the Estimation of Apparent Shear Strength of Composite Materials. Applied Composite Materials 8: 43-62 (2001).

[19] G. Zhou, E. R. Green and C. Morrison. In-plane and interlaminar shear properties of carbon/epoxy laminates. Composites Science and Technology 55(2): 187-193.(1995).

[20] M. Li, R. Matsuyama and M. Sakai. Interlaminar shear strength of C/C-composites The dependence on test methods. Carbon 37(11): 1749-1757. (1999).

[21] P. Feraboli and K. T. Kedward. Four-point bend interlaminar shear testing of uni-

and multi-directional carbon/epoxy composite systems. Composites Part A: Applie Science and Manufacturing 34(12): 1265-1271. (2003).

[22] B.K. Daniels, N.K. Harakas, R.C. Jackson. Short beam shear tests of graphite fiber composites, Fibre Science and Technology 3: 187-208. (1971).

[23] K. Padmanabhan, Kishore. Interlaminar shear of woven fabric Kevlar-epoxi composites in three-point loading. Materials science and engineering A197: 113-118. (1995).

[24] Jiang Zhu, Ashraf Imam, Roger Crane, Karen Lozano, Valery N. Khabashesku, Enrique V. Barrera. Processing a glass fiber reinforced vinyl ester composite with nanotube enhancement of interlaminar shear strength Composites Science and Technology 67: 1509-1517. (2007).

[25] Jaehyun Kim, Masatoshi Shioya, Haruki Kobayashi, Junichi Kaneko, Masahiko Kido. Mechanical properties of woven laminates and felt composites using carbon fibers. Part 2: interlaminar properties.Composites Science and Technology 64: 2231 2238. (2004).

[26] A. Centeno, R. Santamaría, M. Granda, R. Menéndez, C. Blanco Improvement of thermal conductivity in 2D carbon-carbon composites by doping with TiC nanoparticles. Materials Chemistry and Physics 122: 102-107 (2010).

[27] H. Marsh and A. P. Warburton "Catalytic graphitization of carbon using titanium and zirconium." Carbon 14(1): 47-52. (1976).

[28] A. Centeno, R. Santamaría, M. Granda, R. Menéndez, C. Blanco, Development of Ti-doped carbon-carbon composites. J. Mat. Science 44 (19): 2525 (2009). [29] A. Centeno, R. Santamaría, M. Granda, R. Menéndez, C. Blanco. Thermal curing of mesophase pitch: An alternative to oxidative stabilisation for the

development of carbon-carbon composites. Journal of Analytical and Applied Pyrolysis 86(1): 28-32. (2009).

[30] L. M. Manocha and O. P. Bahl. Influence of carbon fiber type and weave pattern on the development of 2D carbon-carbon composites. Carbon 26(1): 13-21. (1988).

[31] C. Blanco, E. Casal, M. Granda, R. Menéndez. Influence of fibre-matrix Interface on the fracture behaviour of carbon-carbon composites. Journal of the European Ceramic Society 23(15): 2857-2866. (2003).

Table Captions

Table 1.- Properties of materials.

Figure Captions

Figure 1.- Optical micrographs corresponding to carbonised materials with 3 densification cycles : (a) undoped matrix; (b) CCTi-C (positions A and B correspond to domains and mosaic texture of the matrix respectively); (c) distribution of TiC in doped matrix and (d) mosaic texture of doped matrix due to TiC agglomeration.

Figure 2.- SEM micrographs of Ti-doped composites with 3 densification cycles: (a) and (b) CCTi-G; (c) Ti-doped carbonised matrix and (d) Ti-doped graphitised matrix

Figure 3.- SEM micrographs of fracture surfaces by shear (XY plane) of materials with 2 densification cycles: (a) CCAR-C and (b) CCTi-C.

Figure 4.- Load-displacement curves of CCAR-G and CCTi-G with 3 densification cycles and corresponding specimens after testing.

Figure 5.- SEM micrographs of fracture surfaces by shear (YZ plane) of materials with 2 densification cycles: (a) CCAR-G and (b) CCTi-G

Figure 6.- SEM micrographs of fracture surfaces by flexure (XZ plane): (a) CCAR-G and (b) CCTi-G.

Table 1.-

Material	n	P_o	P_c	d	Matrix content	ILSS
CCAR-C	1	23	1	1.37	16	21
	2	15	3	1.49	22	56
	3	9	4	1.59	27	61
CCTi-C	1	21	3	1.42	16	27
	2	15	4	1.53	21	67
	3	8	6	1.61	26	70
CCAR-G	1	26	0	1.40	14	-
	2	19	1	1.50	20	8
	3	14	1	1.62	26	27
CCTi-G	1	26	1	1.37	13	-
	2	21	1	1.56	18	18
	3	15	2	1.65	23	28

n, number of densification cycles applied
P_o, open porosity (% vol.)
P_c, close porosity (% vol.)
d, bulk density (g/cm^3)
M, matrix content in the composite (% vol.)
ILSS, interlaminar shear strength (MPa)

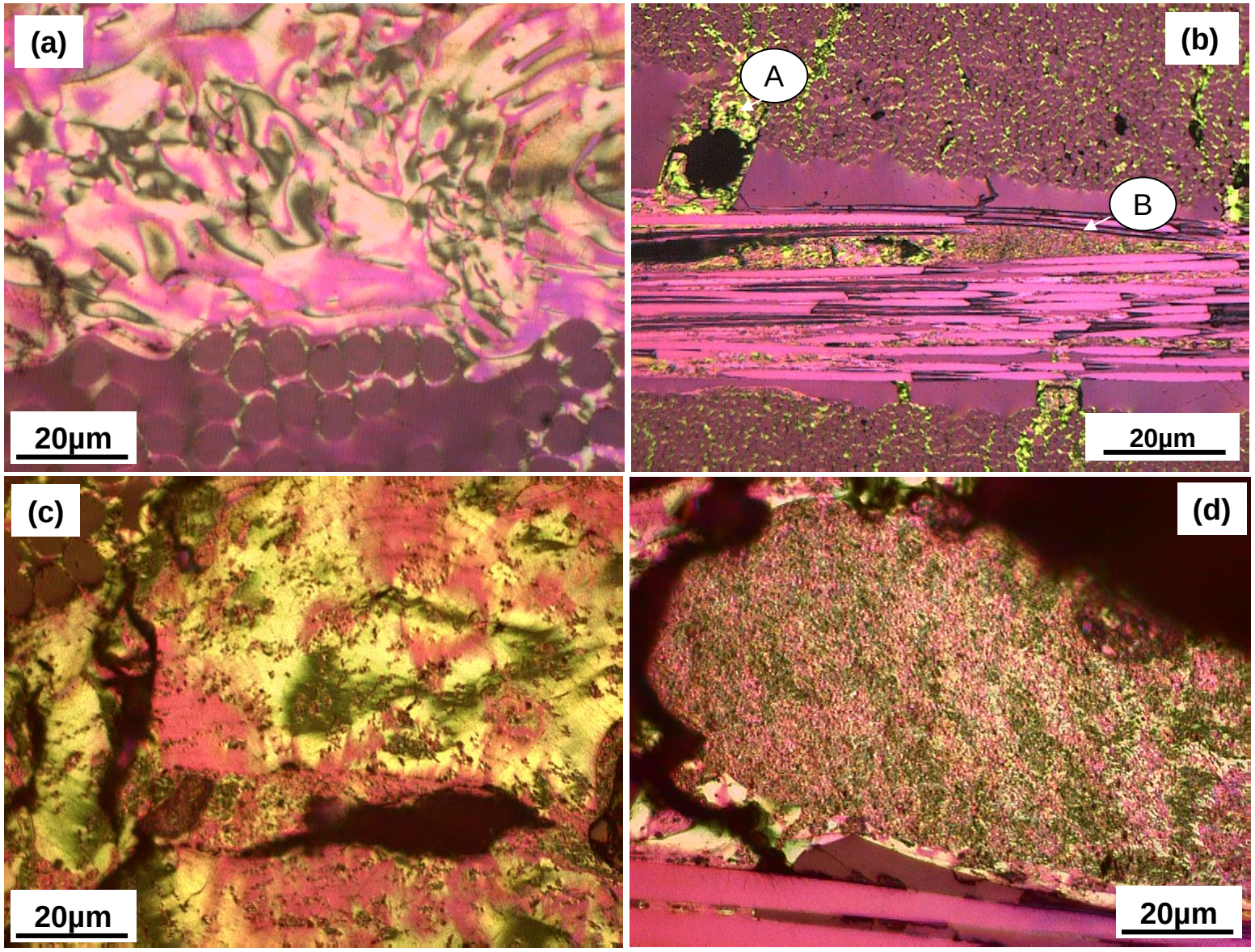

Figure 1.-

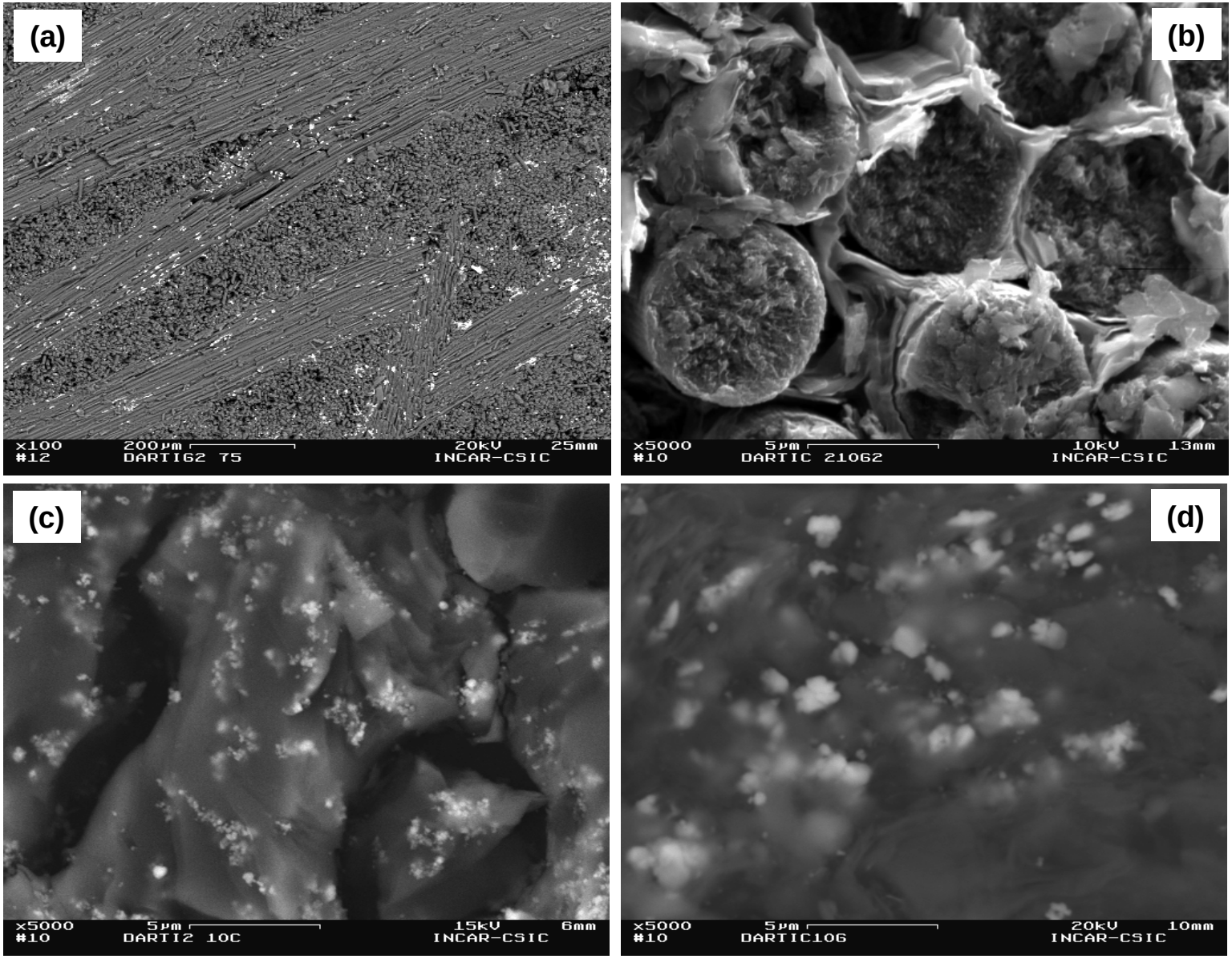
(a)
x100 200µm 20kV 25mm
#12 DARTI62 T5 INCAR-CSIC
(b)
x5000 5µm 10kV 13mm
#10 DARTIC 21062 INCAR-CSIC
(c)
x5000 5µm 15kV 6mm
#10 DARTI2 10C INCAR-CSIC
(d)
x5000 5µm 20kV 10mm
#10 DARTIC106 INCAR-CSIC

Figure 2.-

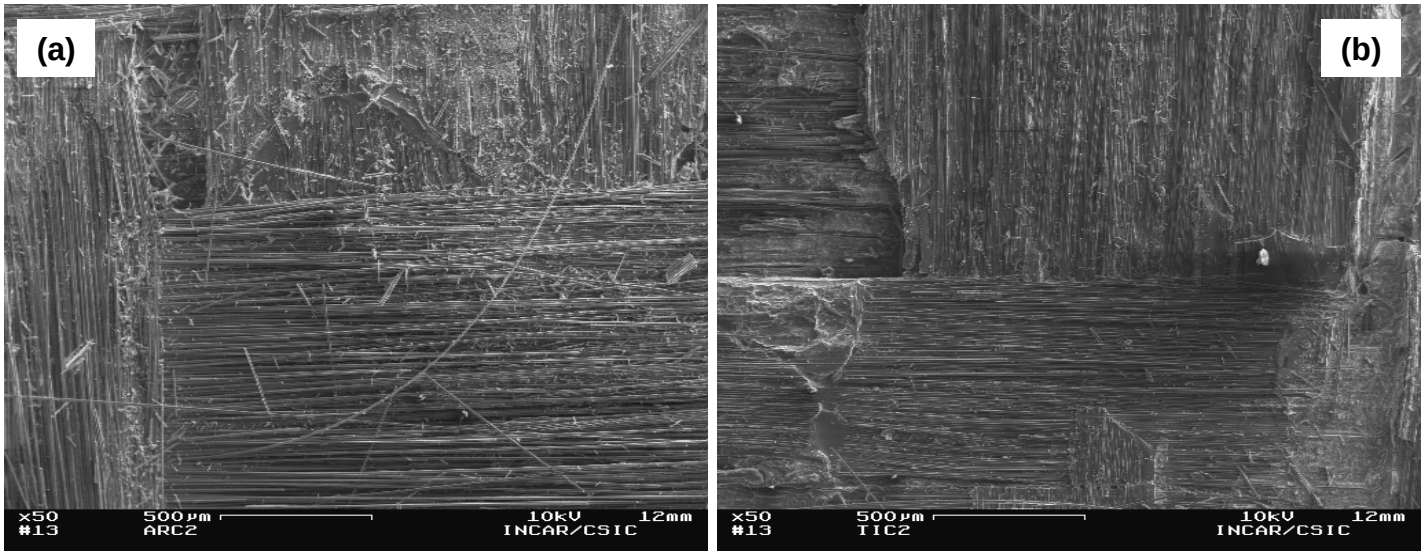
(a)
x50 500µm 10kV 12mm
#13 ARC2 INCAR/CSIC
(b)
x50 500µm 10kV 12mm
#13 TIC2 INCAR/CSIC

Figure 3.-

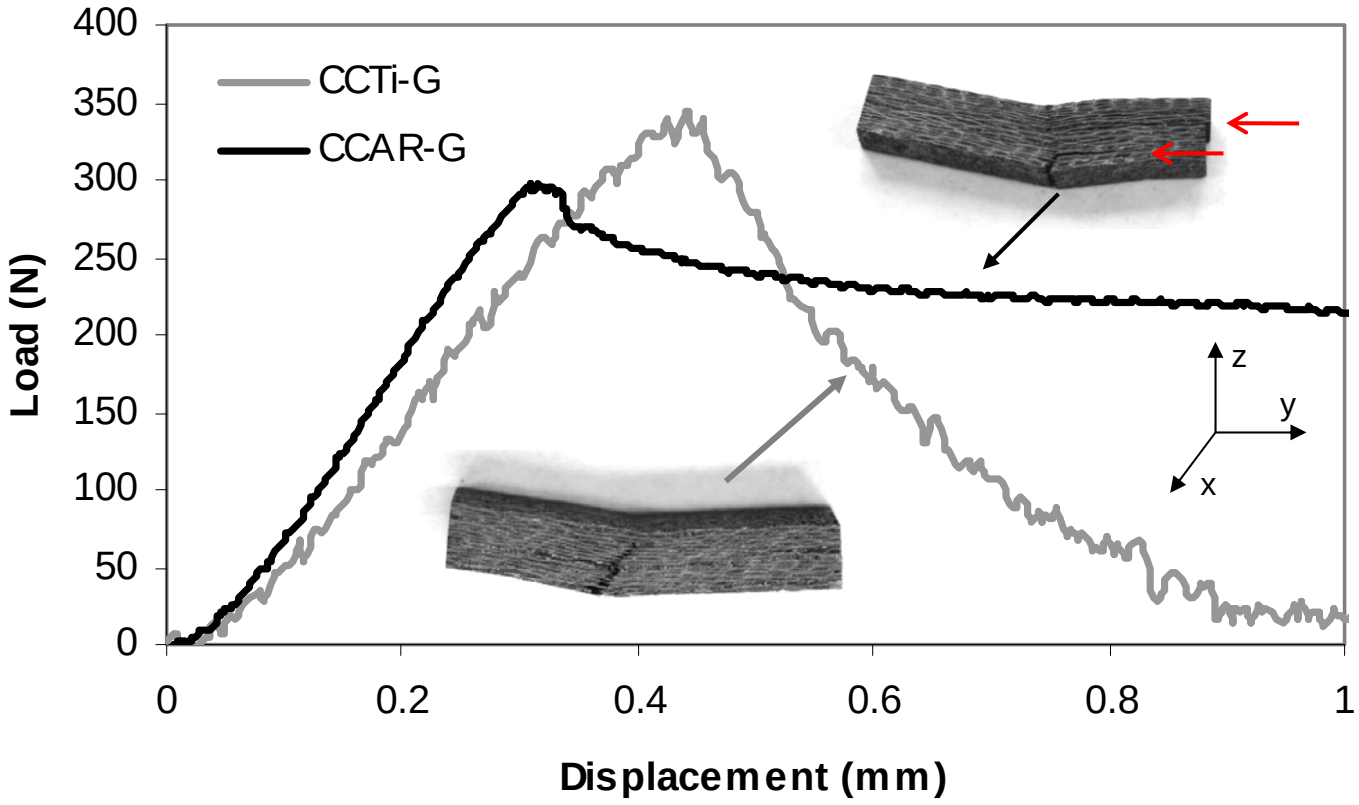
400
350
300
250
200
150
100
50
0
Load (N)
CCTi-G
CCAR-G
0
0.2
0.4
0.6
0.8
1
Displacement (mm)
z
y
x

Figure 4.-

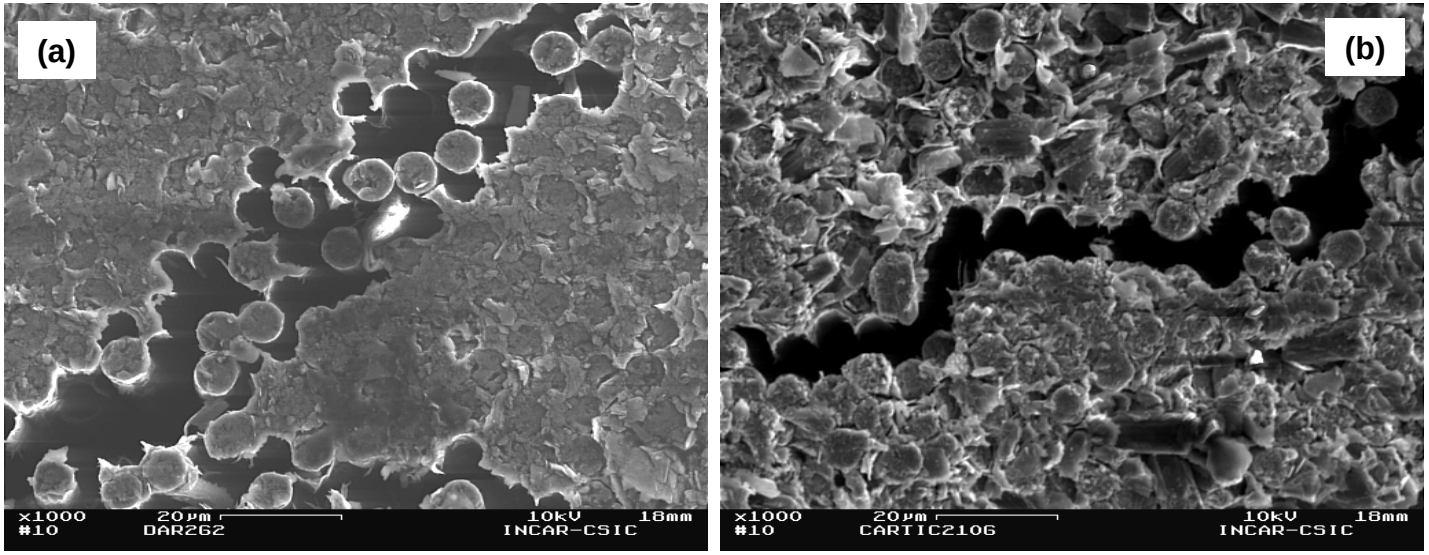
(a)
x1000 20µm 10kV 18mm
#10 DAR2G2 INCAR-CSIC
(b)
x1000 20µm 10kV 18mm
#10 CARTIC210G INCAR-CSIC

Figure 5.-

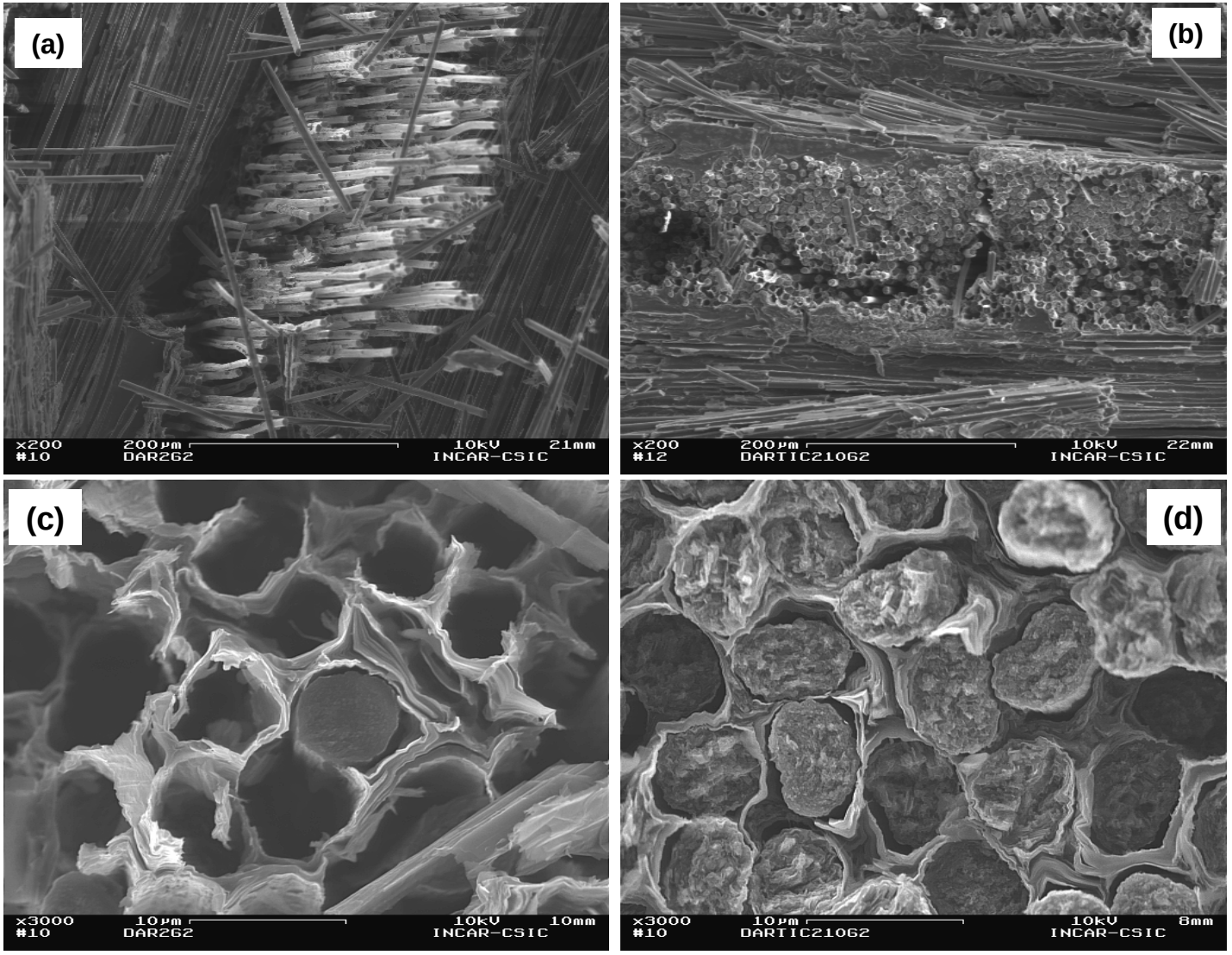
(a)
x200 200µm 10kV 21mm
#10 DAR2G2 INCAR-CSIC
(b)
x200 200µm 10kV 22mm
#12 DARTIC210G2 INCAR-CSIC
(c)
x3000 10µm 10kV 10mm
#10 DAR2G2 INCAR-CSIC
(d)
x3000 10µm 10kV 8mm
#10 DARTIC210G2 INCAR-CSIC

Figure 6.-